

THE KINETICS OF DEHYDROXYLATION OF KAOLINITE

S. A. T. REDFERN

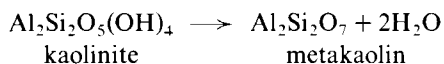
Department of Earth Sciences, University of Cambridge, Downing Street, Cambridge CB2 3EQ

(Received 2 April 1987; revised 20 July 1987)

ABSTRACT: The dehydroxylation of kaolinite has been investigated by isothermal thermogravimetry. Kinetic analysis using the Avrami equation shows that a combination of atomic mechanisms operates throughout the temperature range 734 K to 890 K. An empirical activation energy of 222 kJ mol⁻¹ was calculated from the Arrhenius relationship using rate constants based on diffusion and homogeneous models. The activation energy (E_a) was calculated for a series of degrees of dehydroxylation by the time to a given fraction method, showing an increase in E_a during the early stages of the reaction. The isothermal plots indicate that OH is retained in the final stages of the reaction. The observations are explained in terms of a reaction mechanism in which kaolinite grains dehydroxylate from the edges inwards, parallel to (001).

The dehydroxylation of kaolinite is one of many such reactions that occur within the clay mineral group. In this topotactic transformation, a metastable intermediate phase called metakaolin is formed, this persisting over a temperature range of several hundred degrees. The structure of kaolinite can be thought of as an extended sheet consisting of two components: (i) a sheet of SiO₄ tetrahedra in hexagonal array with bases roughly coplanar and apices pointing in one direction, and (ii) a 'gibbsite' sheet, whose base is formed by apical oxygens of the SiO₄ sheet together with (OH)⁻ ions positioned over the centres of the hexagons of the lower layer, and in which two-thirds of the octahedral sites are occupied by Al ions.

Many investigations have been devoted to the behaviour of kaolinite on heating. Below 670 K, a reversible dehydroxylation process occurs (Fripiat & Toussaint, 1960), and IR hydroxyl bands reappear on cooling. Electron spin resonance studies of Fe³⁺ in the octahedral sheets (Komusinski & Stoch, 1984) reveal that, although there is no major structural change, slight deformations of the octahedral sheet occur below 670 K, reflecting movements of (OH)⁻ groups. Above 670 K kaolinite undergoes an irreversible change involving the loss of constitutional OH, indicated by an endothermic peak in a DTA curve. Work by Stoch & Waclawska (1979), Harman & Horváth (1980), Toussaint *et al.* (1983) and Yeskis *et al.* (1985) indicates that the temperature at which dehydroxylation proceeds at the highest rate varies with original structural state, particle size, density of packing, pressure of H₂O, and other experimental conditions. The transformation can be simply represented:



Early investigations led to a variety of postulated mechanisms explaining the dehydroxylation process, based on both homogeneous and heterogeneous models (Taylor, 1962; Brindley & Nakahira, 1959; Toussaint *et al.*, 1963; Holt *et al.*, 1962). The kinetics of kaolinite

decomposition have been studied extensively by thermogravimetric methods and the results interpreted in terms of a diffusion model as well as first-order kinetics. Brindley *et al.* (1967) favoured a diffusion-controlled process in which dehydroxylation occurs parallel to (001), in agreement with the earlier work of Holt *et al.* (1962). The situation became confused again, however, when Johnson & Kessler (1969) dismissed a diffusion-controlled reaction, concluding that dehydroxylation occurs parallel to (001) and is phase-boundary controlled. Criado *et al.* (1984) showed that the methods of analysis previously used are unable to distinguish between either of these models, but by combining isothermal and non-isothermal techniques they showed the dehydroxylation of kaolinite to be a diffusion-controlled process for reacted fractions up to 0.6. More recently, Stoch (1984) and Suitch (1986) postulated a two-stage mechanism for hydroxyl release. Furthermore, results from NMR spectroscopy (MacKenzie *et al.*, 1985; Watanabe *et al.*, 1987) reveal that around 10% of the hydroxyls persist at the end of the reaction and are difficult to eliminate by dehydroxylation. Brown *et al.* (1985) linked the presence of these stranded hydroxyls to the onset of the higher temperature transformation of metakaolin to mullite and spinel.

All previous kinetic studies have assumed that the rate-controlling process can be described by a single activation energy, which remains constant throughout the transition. The investigation described here employs the \ln 'time to' method of kinetic analysis of isothermal data, as described by Burke (1965), in order to test the validity of this assumption.

EXPERIMENTAL

The kaolinite used was a purified sample from the Lee Moor clay pit on Dartmoor, supplied by English China Clays Ltd. The sample was characterized by TEM, XRD and IR spectroscopy before and after the isothermal experiments. The pseudo-hexagonal morphology of the sample was well developed, TEM revealing an average particle size of 0.4 μm . The powder diffraction data indicated the material to be a well-ordered kaolinite as described by Brindley (1981), with few stacking faults of the 001 planes. The d_{001} spacing was observed not to have varied after dehydroxylation. IR of material before and after heating indicated that significant changes in the octahedral alumina sheets had occurred, as observed by Stubičan (1959).

The kinetics of the dehydroxylation reaction were investigated by isothermal weight loss measurements. The major errors involved in such a technique arise from (i) heat and mass transfer phenomena, which may become pronounced when heating large samples (hundreds of mg), and (ii) difficulties in defining the zero time of the experiment. In order to reduce these errors small samples must be used, and the furnace must reach an equilibrium temperature rapidly. The temperature of the furnace must be accurately stabilized, as the endothermic nature of the reaction may cause self-cooling.

Dry kaolinite was passed through a 52 μm sieve before being heated in a Stanton Redcroft TG 761 thermobalance. This has a furnace capable of reaching 1000°C with a stability of 1°C. The packing density of the sample was kept constant by careful loading of the pan. All isothermal runs were carried out on samples of around 10 mg original mass. Heating was conducted in an N_2 atmosphere with a constant gas flow rate.

Plots of mass loss against time were converted to fraction transformed by measuring the total mass loss at 1000°C after 72 h and assuming 100% reaction at this temperature. The resulting data are shown in Fig. 1.

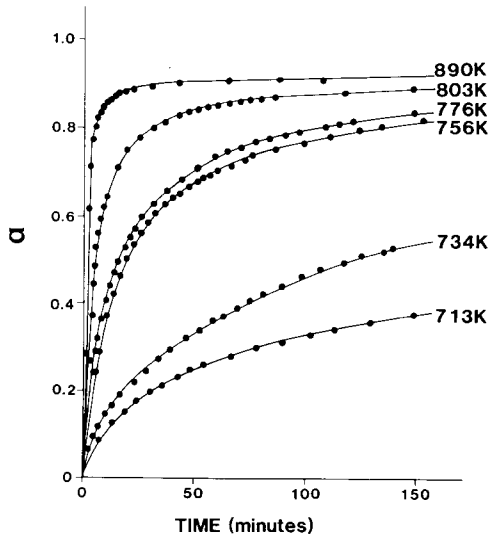


FIG. 1. Isothermal curves for the dehydroxylation of kaolinite.

KINETIC ANALYSIS

There are several approaches to linking a kinetic mechanism to the isothermal weight loss data shown in Fig. 1. All of these kinetic analyses involve the use of the general rate equation:

$$\frac{d\alpha}{dt} = k \cdot f(\alpha) \quad (1)$$

Separation of the variables and integration leads to:

$$g(\alpha) = k \cdot t \quad (2)$$

where α is the reacted fraction at time t , k is the rate constant of the process, and $f(\alpha)$ and $g(\alpha)$ are functions dependent on the mechanism of the reaction. The usual method of kinetic analysis is to test the data against a number of empirical integrated rate equations, find which of these best represents the data, and to calculate values of activation energies for the reaction (see e.g. Criado *et al.*, 1984; Ninan, 1986).

Reactions involving the formation of new domains of a product, and the advancement of a phase boundary, show complex kinetic behaviour and it becomes necessary to resort to empirical solutions of the rate equation. The isothermal kinetics of a wide variety of reactions may be described by the empirical relationship

$$\frac{d\alpha}{dt} = k^m \cdot t^{m-1} \cdot (1 - \alpha) \quad (3)$$

Assuming k and m are independent of α then the integrated rate equation is

$$-\ln(1 - \alpha) = (K \cdot t)^m \quad (4)$$

or

$$\alpha = 1 - \exp(-(K \cdot t)^m) \quad (5)$$

Equation 5 is known as the Johnson–Mehl, or Avrami equation. If kinetic data are plotted as α against $\ln t$ then, for rate curves conforming to the Avrami equation, K fixes the position on the time axis, and the shape of the curve is determined only by m . Fig. 2 shows the data of Fig. 1 plotted in this manner. It can be seen that the curves for 734 K, 756 K, and 776 K are approximately the same shape and may be termed isokinetic.

Taking logarithms of equation 4 we obtain

$$\ln(-\ln(1 - \alpha)) = m \cdot \ln t + m \cdot \ln K \quad (6)$$

Hence, if the reaction obeys the Avrami equation, a set of isokinetic curves would have the same value of m , and similar gradients when plotted as $\ln(-\ln(1 - \alpha))$ vs. $\ln t$. Hancock & Sharp (1972) have shown that the Avrami equation is a generalized equation for the kinetics of solid-state reactions. Kinetic data which follow equations other than (5) also give rise to linear plots in the range 0.15–0.50.

The data from the dehydroxylation of kaolinite are plotted as a ‘ $\ln \cdot \ln$ ’ graph in Fig. 3. The gradients of these series of lines as determined by least-squares linear regression are given in Table 1. The value of these gradients is characteristic of the rate-determining kinetic mechanism operating at that temperature.

Again we see the isokinetic character of the runs at the lowest three temperatures. Comparison of these values with the values of m for various solid-state reaction rate equations, as given by Hancock & Sharp (1972), indicates that the behaviour for these lowest three runs is intermediate between that of diffusion-controlled and first-order models for values of $\alpha \leq 0.5$. For the lowest temperature run the data agree with a diffusion-controlled model such as $D_2(\alpha)$ of Brindley *et al.* (1967), but the values of m increase, approaching those of first-order rate equations, as the temperature is increased. At the higher temperature of 803

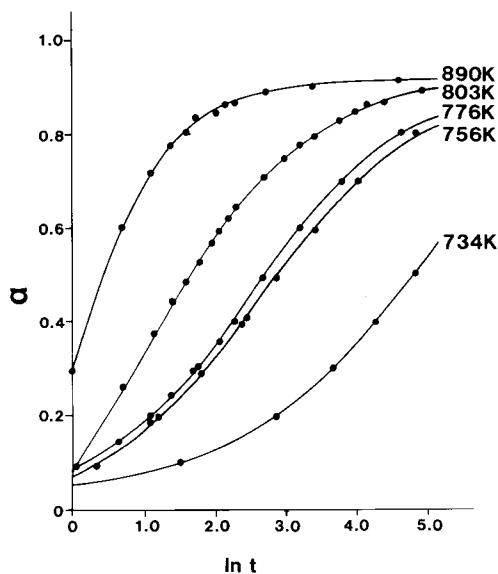


FIG. 2. Reaction curves for kaolinite, showing agreement with the Avrami equation.

TABLE 1. Results of 'ln.ln' analysis for the isothermal data of Fig. 1.

T/K	m	r
890	1.5	0.9782
803	1.0	0.9802
776	0.7	0.9999
756	0.7	0.9969
734	0.6	0.9993

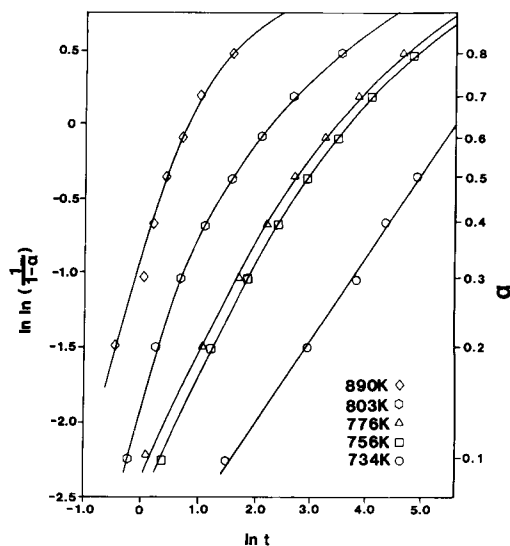


FIG. 3. 'ln.ln' plot of the kaolinite kinetic data.

K, m corresponds to that of a first-order model, and at 890 K m has a value that does not correspond to any of the models considered by Hancock & Sharp (1972). These results agree with the findings of Craido *et al.* (1984) who explained the higher temperature behaviour as heat-mass transfer controlled due to high reaction rates. It should also be noted that at such high reaction rates, errors in defining the start time of the reaction become more significant.

The deviation from linearity of the 'ln.ln' plots for $\alpha > 0.5$ is a result of the reaction equations being non-identical to the Avrami equation, and was predicted by Hancock & Sharp (1972).

Determination of activation energies

The temperature dependence of the rate constant for most reactions obeys an Arrhenius type equation. The empirical activation energy, E_a , and frequency factor, A are defined by the equation

$$k = A \cdot \exp(-E_a/RT) \quad (7)$$

E_a and A may only be identified with the activation energy for a basic atomic event in the case of a singly activated process. Otherwise they are purely empirical values corresponding to complex multiple atomic events. The logarithmic form of the Arrhenius equation for k is

$$\ln k = \ln A - E_a/RT \quad (8)$$

There are a number of methods by which E_a and A may be calculated from these relations. Most commonly, values of k are determined at various temperatures from the integrated rate equations for the reaction. If E_a and A are constant, $\ln k$ is proportional to $1/T$, with gradient $-E_a/R$ and intercept $\ln A$.

This procedure has been carried out for the isothermal runs at 803 K, 776 K, and 734 K. Fig. 4 shows the relationship between $\ln k$ and $1/T$ for an homogeneous first-order

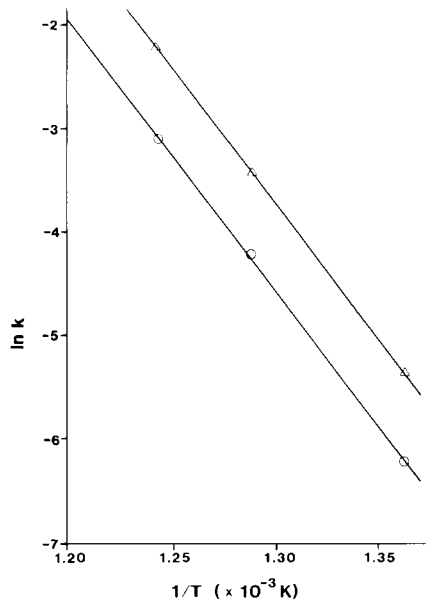


FIG. 4. Arrhenius plot of the kaolinite kinetic data.

mechanism and a diffusion-controlled mechanism, the two possible rate-controlling mechanisms inferred from the values of m found above. As can be seen, these plots have very similar gradients and both give the same activation energy of 222 kJ mol^{-1} .

This method has the disadvantage that it fails to show any possible variation in the activation energy as a function of α . Generally it may also yield a value of E_a dependent on the function $g(\alpha)$ selected empirically and used to calculate k , although this does not appear to be the case for kaolinite.

In complex processes involving many atomic events the contribution made by individual events may vary as the reaction proceeds. To determine any changes in the kinetic controlling mechanism during the dehydroxylation, the activation energy E_a must be determined independently of the empirical functions $g(\alpha)$. Burke (1965) showed that by rewriting equation (1), the time, t_Y , for a given fraction $\alpha = Y$ to transform is:

$$t_Y = k^{-1} \int_0^Y f^{-1}(\alpha) d\alpha \quad (9)$$

Values of t_Y were collected for a series of temperatures. Provided that $f(\alpha)$ does not vary over the temperature range studied, the integral is constant. Thus t_Y is proportional to k^{-1} , and from (7):

$$t_Y \propto A^{-1} \cdot \exp(E_a/RT) \quad (10)$$

$$\ln t_Y = \text{const} - \ln A + E_a/RT \quad (11)$$

In Fig. 5 the data are plotted as $\ln t_Y$ against $1/T$. The slope is E_a/R if E_a and A are independent of temperature. The slope of the graphs varies as temperature changes, due to non-isokinetic behaviour. Between 734 K and 776 K, however, the mechanism approaches isokinetic behaviour, and the 803 K 'ln. ln' plot does not deviate greatly in gradient from the 776 K plot for values of α greater than 0.2. Therefore the activation energies at values $\alpha = Y$

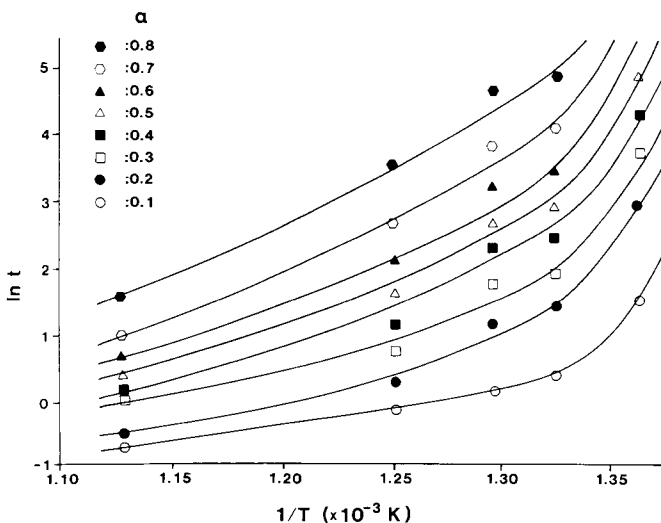


FIG. 5. $\ln t$ vs. $1/T$ for α from 0.1 to 0.8.

have been calculated from groups of points corresponding to (734 K, 756 K, 776 K, 803 K), (734 K, 756 K, 776 K), and (756 K, 776 K, 803 K), allowing the determination of the evolution of activation energy with reaction coordinate, as shown in Fig. 6. This shows that the average activation energy from the start of the reaction increases until $\alpha = 0.4$. The implication of this plot is that the reaction starts with a low activation energy, and very soon (before $\alpha = 0.1$) another mechanism with a higher activation energy becomes the rate-controlling process for dehydroxylation. This second process has an activation energy of between 200 and 250 kJ mol^{-1} .

DISCUSSION

Investigation of the kinetics of dehydroxylation of kaolinite by ln. ln analysis shows that a diffusion-controlled process dominates below ~ 780 K, and the controlling mechanism changes at higher temperatures. This may be a result of experimental difficulties in defining the start time for runs with high reaction rates, but may also be explained in terms of the

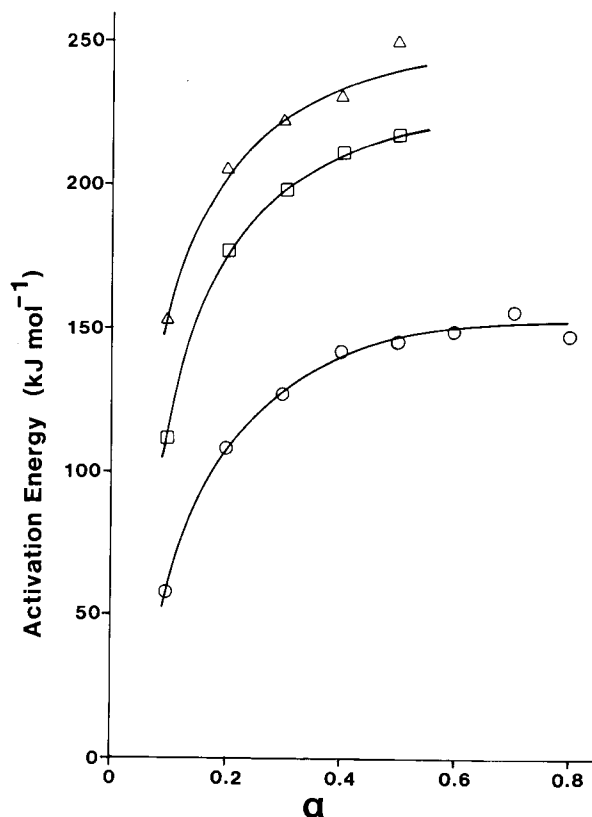


FIG. 6. Activation energies calculated by the ln 'time to' method, showing the rapid increase from small values at the start of the reaction. Calculated from three sets of data in Fig. 5: Δ = 734 K, 756 K, 776 K, \square = 734 K, 756 K, 776 K, 803 K, \circ = 756 K, 776 K, 803 K.

increased diffusion rate at these elevated temperatures, with some other slower kinetic process then controlling the reaction rate. The empirical activation energy derived from the Arrhenius equation is the same when calculated using a diffusion rate constant, and a homogeneous rate constant. This agrees with the results obtained by Criado *et al.* (1984), who concluded that the activation energy obtained from the Arrhenius law is independent of the kinetic function $g(\alpha)$.

The activation energies calculated by the time to a given fraction method show that the activation energy is low at the start of the reaction ($\alpha < 0.1$) and then increases to a much higher value. Holt *et al.* (1962) and Toussaint *et al.* (1963) showed that the activation energy increases with increasing H_2O pressure. The increase in activation energy observed in this analysis may be explained as a built up of intergrain vapour pressure as the reaction proceeds. Goss (1987) points to the retention of water within the porous structure of goethite as being an important control on the transformation to hematite, a similar dehydration reaction.

Another possible reaction mechanism which also explains the observed variation of activation energy is that described by Horváth & Kranz (1980) in which the reaction proceeds

from the edges of the grains inwards parallel to the (001) planes. At the first stages of the reaction there is a low activation energy because OH groups at the edges of the plates may escape without diffusion through the grain. Stoch & Wacławska (1979) found that smaller grain size results in lower activation energies for the same reason. If metakaolin formed in this manner closes interlamellar channels, regions of kaolinite are effectively isolated within the grains, resulting in a much higher activation energy for dehydroxylation of these regions. In this case the regions of kaolinite would still diffract X-rays as observed, to give weak reflections with unchanged spacing. Recent NMR results (Otero-Arean *et al.*, 1982; MacKenzie *et al.*, 1985; Watanabe *et al.*, 1987) have been interpreted in a similar manner. Hence the rapid increase in activation energy observed by this kinetic analysis supports a model of dehydroxylation parallel to (001) in which residual hydroxyl groups become stranded, leaving unreacted portions of kaolinite within the metakaolin.

The sharp decrease in reaction rate above ~80% transformed seen in Fig. 1 may also be explained by the inward progression of the reaction from the plate edges, and the higher activation energy in the final stages of dehydroxylation.

ACKNOWLEDGMENTS

The author thanks English China Clays for supplying the kaolinite and Dr Andrew Putnis for reviewing the manuscript. This is Cambridge Earth Sciences contribution no. 1019.

REFERENCES

- BRINDLEY G.W. & NAKAHIRA M. (1959) The kaolinite–mullite reaction series; I, II, III. *J. Am. Ceram. Soc.* **42**, 311–314, 314–318, 319–324.
- BRINDLEY G.W., SHARP J.H., PATTERSON J.H. & NARAHARI ACHAR B.N. (1967) Kinetics and mechanism of dehydroxylation processes: I, temperature and vapor pressure dependence of dehydroxylation of kaolinite. *Am. Miner.* **52**, 201–211.
- BRINDLEY G.W. & BROWN G. (1980) *Crystal Structures of Clay Minerals and their X-Ray Identification*. Mineralogical Society, London.
- BROWN I.W., MACKENZIE K.J.D., BOWDEN M.E. & MEINHOLD R.H. (1985) Outstanding problems in the kaolinite–mullite reaction sequence investigated by ^{29}Si and ^{27}Al solid-state nuclear magnetic resonance: II, high-temperature transformation of metakaolinite. *J. Am. Ceram. Soc.* **68**, 298–301.
- BURKE J. (1965) *The Kinetics of Phase Transformations in Metals*. Pergamon Press, Glasgow.
- CRiADO J.M., ORTEGA A., REAL C. & TORRES DE TORRES E. (1984) Re-examination of the kinetics of dehydroxylation of kaolinite. *Clay Miner.* **19**, 653–661.
- FRIPIAT J.J. & TOUSSAINT F. (1960) Prehydroxylation state of kaolinite. *Nature* **186**, 627.
- GOSS C.J. (1987) The kinetics and reaction mechanism of the goethite to hematite transformation. *Mineral. Mag.* **51**, 437–451.
- HANCOCK J.D. & SHARP J.H. (1972) Method of comparing solid-state kinetic data and its application to the decomposition of kaolinite, brucite and BaCO_3 . *J. Am. Ceram. Soc.* **55**, 74–77.
- HARMAN M. & HORVÁTH I. (1980) Relations between the morphology of particles in structurally differently ordered kaolinites and the kinetics of their dehydroxylation. *Geol. Zbor. Geol. Carpath.* **31**, 115–124.
- HOLT J.B., CUTLER I.B. & WADSWORTH M.E. (1962) Rate of dehydroxylation of kaolinite in vacuum. *J. Am. Ceram. Soc.* **45**, 133–136.
- HORVÁTH I. & KRANZ G. (1980) A thermoanalytical study of high-temperature dehydration of kaolinites with various structural arrangements. I. The changes in weight during dehydroxylation. *Silikáty* **24**, 149–156.
- JOHNSON H.B. & KESSLER F. (1969) Kaolinite dehydroxylation kinetics. *J. Am. Ceram. Soc.* **52**, 199–204.
- KOMUSINSKI J. & STOCH L. (1984) Dehydroxylation of kaolinite group minerals: an ESR study. *J. Thermal Anal.* **29**, 1033–1040.
- MACKENZIE K.J.D., BROWN I.W.M., MEINHOLD R.H. & BOWDEN M.E. (1985) Outstanding problems in the kaolinite–mullite reaction series investigated by ^{29}Si and ^{27}Al solid-state nuclear magnetic resonance: I, metakaolinite. *J. Am. Ceram. Soc.* **68**, 293–297.

- NINAN K.N. (1986) Thermal decomposition kinetics. Part XIV. Kinetics and mechanism of isothermal decomposition of calcium oxalate monohydrate and correlation with sample mass. *Thermochim. Acta* **98**, 221–236.
- OTERO-AREAN C., LETELLIER M., GERSTEIN B.C. & FRIPIAT J.J. (1982) Protonic structure of kaolinite during dehydroxylation studied by proton nuclear magnetic resonance. *Bull. Mineral.* **105**, 499.
- STOCH L. (1984) Significance of structural factors in dehydroxylation of kaolinite polytypes. *J. Thermal Anal.* **29**, 919–931.
- STOCH L. & WACLAWSKA I. (1979) The kinetics of kaolinite dehydroxylation. *Polska Acad. Nauk. Prace Min.* **59**, 59–79.
- STUBIČAN V. (1959) Residual hydroxyl groups in the metakaolin range. *Mineral. Mag.* **32**, 38–52.
- SUITCH P.R. (1986) Mechanism for the dehydroxylation of kaolinite, dickite, and nacrite from room temperature to 455°C. *J. Am. Ceram. Soc.* **69**, 61–65.
- TAYLOR H.F.W. (1962) Homogeneous and inhomogeneous mechanisms in the dehydroxylation of minerals. *Clay Miner. Bull.* **5**, 45–55.
- TOUSSAINT F., FRIPIAT J.J. & GASTUCHE M.C. (1963) Dehydroxylation of kaolinite. I. Kinetics. *J. Phys. Chem.* **67**, 26–30.
- WATANABE T., SHIMIZU H., NAGASAWA K., MASUDA A & SAITO H. (1987) ²⁹Si- and ²⁷Al-MAS/NMR study of the thermal transformations of kaolinite. *Clay Miner.* **22**, 37–48.
- YESKIS D., KOSTER VAN GROOS A.F. & GUGGENHEIM S. (1985) The dehydroxylation of kaolinite. *Am. Miner.* **70**, 159–164.